

Empirical Relationship between Particulate Matter and Aerosol Optical Depth over Northern Tien-Shan, Central Asia

Boris B. Chen <sup>(a)\*</sup>

Leonid G. Sverdlik <sup>(a)</sup>

Sanjar A. Imashev <sup>(a)</sup>

Paul A. Solomon <sup>(b)</sup>

Jeffrey Lantz <sup>(c)</sup>

James J. Schauer <sup>(d)</sup>

Martin M. Shafer <sup>(d)</sup>

Maria S. Artamonova <sup>(e)</sup>

Greg Carmichael <sup>(f)</sup>.

(a) Kyrgyz-Russian Slavic University, 44 Kievskaya Str., Bishkek 720000, Kyrgyz Republic,

(b) U.S. EPA, Office of Research & Development, Las Vegas, NV 89119 USA,

(c) U.S. EPA, Office of Radiation and Indoor Air, Las Vegas, NV 89119 USA,

(d) Wisconsin State Laboratory of Hygiene, University of Wisconsin, 660 North Park St, Madison, WI 53706, USA, Environmental Chemistry and Technology Program, 660 North Park St, University of Wisconsin, Madison 53706, USA,

(e) Institute of Atmospheric Physics, 109017 Moscow, Russia,

(f) Department of Chemical & Biochemical Engineering, the University of Iowa, Iowa City, IA 52242.

\*: Corresponding Author:

Email: [lidar@istc.kg](mailto:lidar@istc.kg)

Address: Kyrgyz-Russian Slavic University, 44 Kievskaya Str., Bishkek 720000, Kyrgyz Republic

Telephone: 996-312-431-197

Fax: 996-312-431-171

## Abstract

Measurements were obtained at two sites in northern Tien-Shan in Central Asia during a one year period beginning July 2008 to examine the statistical relationship between aerosol optical depth (AOD) and of fine (PM<sub>2.5</sub>, particles less than 2.5  $\mu\text{m}$  aerodynamic diameter [AD]) and coarse (PM<sub>Coarse</sub>, particle between 2.5 and 10  $\mu\text{m}$  AD) mass concentrations and composition. The measurements represent the first extended particulate matter measurements in the northern Tien Shan region of Central Asia. A sun photometer (Microtops II) was used to measure AOD from the surface, which is widely used aerosol monitoring technique that is used in the AERONET network. In parallel, less routine measurements of continuous hourly PM<sub>2.5</sub> data were obtained with the TEOM/FDMS whereas daily average PM<sub>2.5</sub> and PM<sub>10</sub> were obtained using URG-3000ABC samplers. Daily samples were collected on an every other day basis throughout the year. Since clouds interfere with the AOD measurement, a cloud screening procedure, based on LIDAR measurements was applied to the AOD data and cloud impacted days were removed from the AOD data set. Depending on the season, the correlation coefficient ( $r$ ) varied from 0.56 up to 0.87. Higher correlation coefficients between PM<sub>2.5</sub> mass and AOD were observed during the spring and autumn periods and appeared to result from the transport of Asian dust (desert crustal material) particles from outside the area. One of the main source areas was the Taklimakan desert located in northwestern China. Linear regression results between AOD and PM<sub>2.5</sub> are presented that allow for an estimate of PM<sub>2.5</sub> mass concentrations at the surface based on the AOD data, which can be used to help interpret AOD measurements made in Central Asia and potentially other regions of the world.

Keywords: PM<sub>2.5</sub>, PM<sub>Coarse</sub>; aerosol optical depth, Central Asia, dust, transport.

## 1. Introduction

Atmospheric particulate matter (PM) influences climate (IPCC, 2007; Ramanathan et al., 2001) and has been shown to result in adverse health effects (Pope and Dockery, 2006; Heo et al., 2009; Solomon et al., 2011). As a result, systematic ground and satellite measurements have been undertaken to obtain improved information on atmospheric PM and composition at high temporal and spatial resolution. A major source of particles in the atmosphere comes from the world's deserts. Approximately 500 million people or 8 % of the planet's population lives in and near deserts that occupy almost 20 % of the earth surface (UNEP, 2006). These deserts are the main natural source of dust in the atmosphere, which can be transported over long distances from source regions and even between continents. For example, dust from the Sahara and Arabian deserts is transported in middle latitudes of the troposphere by zonal west-east flow patterns through mountain ridges of Central Asia to Korea and Japan (Park et al., 2005;

Lee et al., 2006; McKendry et al., 2007). Asian dust from the Gobi and Taklimakan deserts in East Asia reaches both the Far East and North America (Uno et al., 2008; Husar et al., 2001; Fischer et al., 2009; Lee et al., 2010). Liu et al. (2008) and Lee et al. (2010) indicate that many regions of the world are under the influence of desert dust approximately 50 % of time.

Great attention has been given to air quality assessments in the USA, Southeast Asia, and Western Europe on the basis of PM<sub>2.5</sub> (particles less than and equal to 2.5  $\mu\text{m}$  aerodynamic diameter, AD) ground-level measurements. However providing similar surface-based PM measurements in other regions of the world is limited due to lack of observations. Therefore, there is great interest in estimating PM mass concentrations on the basis of satellite passive optical sensing or remote sensing from the surface based aerosol optical depth and subsequent use of proportionality coefficients between AOD and PM to estimate aerosol concentrations at ground level (Kokhanovsky et al., 2008; Van Donkelaar et al., 2009). The relation between PM<sub>2.5</sub> and AOD depends on many factors and usually changes significantly, even for data obtained at the same site during the year due to variations in source impacts and meteorology. Empirical studies of the relationship between PM<sub>2.5</sub> and AOD have been reported in various regions of the world (Gupta et al., 2006; Hoff and Christopher, 2009; Kugmierczyk-Michulec, 2010), in the USA (Wang and Christopher, 2003; Engel-Cox et al., 2004; Zhang et al., 2009), in a densely populated area and industrially developed regions of Asia (Kumar et al., 2007; Mukai et al., 2008; Wang et al., 2010), and in Europe (Kacenenbogen et al., 2009; Schaap et al., 2009; Pelletier et al., 2007; Dinoi et al., 2010). Nevertheless, as it is noted in Schaap et al., (2009), relationships between AOD and PM obtained on local scales, cannot be easily extrapolated to other areas because of variations in source types, PM composition, and meteorology. Therefore continued research is needed to quantify PM-AOD relationships in various regions of the world, but especially in locations where few surfaced-based PM measurements have been obtained to date.

Central Asia is a region with very limited experimental data on direct surfaced-based measurements of PM concentrations. The results reported here begin to address this lack of information by providing the first direct measurements and analysis of the relationship between PM<sub>2.5</sub> and AOD in Central Asia. These measurements also are part of a larger study designed to obtain first time measurements of PM mass and detailed chemical composition in this region. This area is highly influenced by pollution from regional dust sources (Taklimakan desert and Aral Sea basin) and transport from Near-Eastern dust. Seasonality of the AOD-PM relationship and the role of mineral dust also are examined in this one year study.

## 2. Location, instruments and measurements

Measurements were obtained at two locations in Kyrgyzstan located south of Kazakhstan, west of China, and north of Tajikistan (Figure 1). Brief site descriptions are given in Table 1. The study was conducted

for a one-year period from July 2008 through June 2009. One site was located in north central Kyrgyzstan, south of Bishkek the capital of Kyrgyzstan; the other was located approximately 325 km south southeast of Bishkek near the city of Karakol. The latter site was named the LIDAR site due to the collocated LIDAR system located there. Measurements were obtained simultaneously obtained at both sites as described in Table 2.

One of the main requirements in selecting sites for this study was their altitude above the sea level and their distance away from urban areas, both of which minimized the influence from local PM sources, as the project was focused on the study of long-range and transboundary pollution transport within Central Asia and from Central Asia eastward. The sites also had existing infrastructure and staff, which allowed for the collection of samples throughout the year.

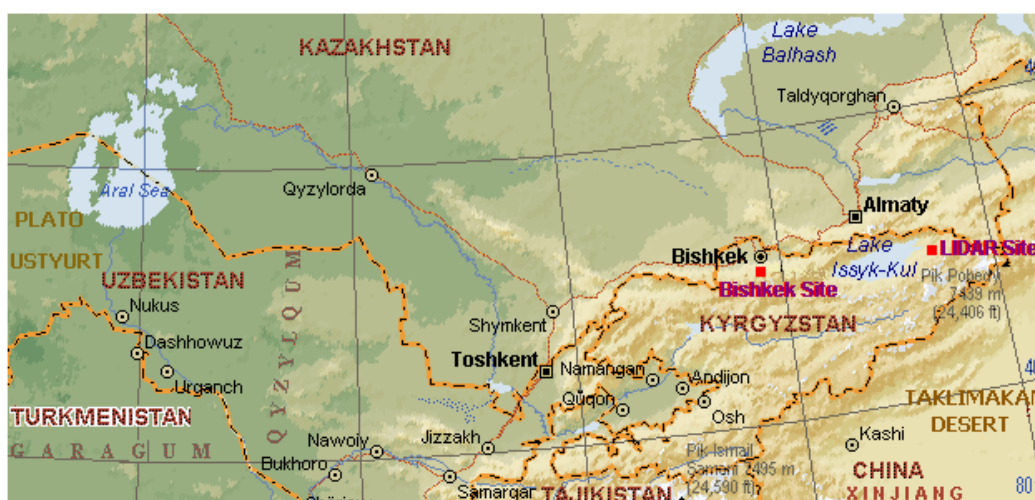


Figure 1. Location of the LIDAR and Bishkek monitoring sites.

Table 1. Experimental site locations

Site	Location / Sampling Began	Latitude	Longitude	Altitude
<b>BISHKEK</b>	35 Km South of Bishkek, On Grounds of Geophysical Research Station of the RAS in Bishkek city / May 01, 2008	N 42,68	E 74,69	1750 m
<b>LIDAR</b>	20 Km North of Karakol On Grounds of LIDAR Station Teplokluchenka / May 02, 2008	N 42,47	E 78,53	2000 m

Table 2. Specification of equipment and measured parameters

Instrument (Manufacturer)	Measurable Quantity and Components	Averaging Time /Sample Collection Frequency
Automatic Ambient Air Particulate Matter Monitor 1400 TEOM/8500 FDMS (Thermo Scientific)	Total PM <sub>2.5</sub> Mass ( $\mu\text{g}/\text{m}^3$ ), Non-volatile PM <sub>2.5</sub> Mass ( $\mu\text{g}/\text{m}^3$ ), Volatile PM <sub>2.5</sub> Mass ( $\mu\text{g}/\text{m}^3$ )	Hourly / Every day, Continuous

Aerosol Filter Sampler URG-3000ABC (URG CORPORATION)	Parallel PM10 and PM2.5 Aerosols Collected on Teflon (47mm) and Quartz (47mm) Filters for Detailed Chemical Characterization	24-hr / Every Other Day
Sun Photometer Microtops II (SOLAR Light Co. Inc.)	Direct solar radiation and AOD at five wavelengths (340, 380, 500, 675, 870nm), hand-held	Daily average / Every 1-hr each cloud-free day from 02:00UTC to 11:00UTC
Stationary scanning Aerosol Backscatter Multiwavelength LIDAR with Raman channel	Aerosol backscatter (355, 532, 1064nm), Raman scattering (387nm), Depolarization (532nm)	Not less 0.5-hr / Standard measurements twice a week, Event Basis
Automatic Meteorological Station (K.Fischer company)	Temperature, Relative Humidity, Pressure, Irradiance, Wind Direction and Wind Speed	Hourly / Every day, Continuous

Remote sensing, from the surface, of aerosol optical depth (AOD) was obtained using a Microtops II sun photometer (MII). The measurement accuracy of the Microtops II (SN 12568 and 12569) instrument was less than 0.02 (Ichoku et al., 2002). Additionally, comparison of the Microtops II to a sun photometer CIMEL CE 318-2 (CIMELElectronique, France) located at the AERONET Issyk-Kul Scientific Station (AErosol RObotic NETwork; <http://croc.gsfc.nasa.gov/aeronet/>) approximately 80 km to the NW of the LIDAR site, showed a high correlation ( $r^2 > 0.70$ ).

A tapered element oscillating microbalance with the filter dynamics measurement system (TEOM/FMDS) was employed at both sites to provide continuous, hourly-average measurements of PM2.5 mass concentrations. Flow rates were verified using a DC-2 air flow calibrator (BIOS International Corporation, Butler, NJ), as well, leak checks were performed on a regular basis to help ensure the validity of the data. The TEOM/FDMS was nonoperational at the Bishkek site from 17 October until 31 December 2008, and therefore PM2.5 data from the URG-3000ABC sampler (described below) were used in the analysis. In addition, the FDMS failed to work at Bishkek so the mass measurements represents primarily non-volatile PM, whereas the TEOM at the LIDAR site operated as planned and provided total PM2.5 mass, which includes volatile as well as non-volatile components in the mass measurement (Solomon and Costas, 2008).

A URG-3000ABC sampler (University Research Glassware) was located at both sites to obtain daily samples of PM2.5 and PM10 (particles with diameters less than 10  $\mu\text{m}$  AD) for subsequent determination of mass and detailed chemical analysis on an every other day sampling schedule. Coarse particle mass (PMCoarse), in the size range between 2.5  $\mu\text{m}$  and 10  $\mu\text{m}$  AD was determined by the difference between PM10 and PM2.5. Before sampling, flow rates were verified using a rotameter (model P-03269-80) and a series of leak checks were performed. PM mass was determined by the difference between pre- and post-collection by weighing the Teflon filters on a micro-balance after equilibration under controlled temperature and relative humidity (Federal Register 2006). Independent audits of the TEOM and URG samplers were carried out by the U.S. Environmental Protection Agency (EPA) at the beginning and end of the study. Except for the TEOM at Bishkek, which was not operational

at the time of the initial audit, all samplers met EPA's guidelines for flow rate, temperature, and pressure, as applicable to each sampler. All samplers met EPA's guidance for these parameters at the final audit. Comparison of PM<sub>2.5</sub> mass measured by the URG-3000ABC to 24-hour average values of PM<sub>2.5</sub> mass obtained by the TEOM/FDMS showed a high correlation ( $r^2 = 0.97$ ).

The LIDAR site also was equipped with a multichannel Raman and polarization LIDAR with three working wavelengths that was intended for sensing of aerosol in the planetary boundary layer (PBL) and free troposphere up to 10-12 km above ground level (Chen et al., 2004). Raman measurements at 387 nm were taken after sunset. This method allows for the determination of aerosol extinction coefficients in the PBL at night as well as during the day. Simultaneous LIDAR and sun photometer measurements were obtained on 103 days out of the year.

AOD measurements can be distorted by clouds, including thin clouds. Two approaches were employed to verify the presence of clouds. First for visible clouds, site operators used a special code to describe the condition of the atmosphere during the moment of the measurement. Secondly, LIDAR data were used as an auxiliary method to identify optically thin clouds in the free troposphere not visible to an observer. The procedure of clouds screening was based on the method of Smirnov et al. (2009) that has been used to data quality check the Maritime Aerosol Network (MAN).

The cloud filtration procedure was applied to all daytime hourly measurements. Measurements included a series of 5 scans ( $AOD_i$ , where  $i = 1, 2, \dots, 5$ ). For each series a minimal value of aerosol optical depth ( $AOD_i^{min}$ ) was calculated. Data with a deviation from the minimum value ( $AOD_i^{min}$ ) that exceeded 30 % ( $AOD_i/AOD_i^{min} - 1 < 0.3$ ) for each wavelength were removed, e.g., the sun photometer was not aimed towards the sun (Ichoku et al., 2002). Scans within the series ( $AOD_i$ ) were considered cloud-free if they met the following conditions (Smirnov et al., 2009): a)  $AOD_i^{min} < 0.4$  and  $(AOD_i - AOD_i^{min}) < 0.02$ ; b)  $AOD_i^{min} \geq 0.4$  and  $(AOD_i - AOD_i^{min}) < AOD_i^{min} \times 0.05$ . Removal of outliers due to cloud screening varied in different months from 10 to 30 %. Hourly average values ( $AOD_h$ ) were computed on all cloud-free  $AOD_i$ , and daily average values for the month were computed as a simple average of all  $AOD_h$ .

Time series of AOD were used for establishing a statistical relation between  $AOD_{500}$  (aerosol optical depths at a wavelength of 500 nm) and the mass concentration of PM<sub>2.5</sub> and PM<sub>Coarse</sub>. The analysis in this paper used PM<sub>Coarse</sub> instead of PM<sub>10</sub> since PM<sub>10</sub> already includes PM<sub>2.5</sub>. This approach allowed for the influence of coarse and fine particles separately on AOD.

### 3 Results and Discussion

#### 3.1 Seasonal variations of AOD by sun photometer and PM relationships

Yearly averaged AOD<sub>500</sub> at the Bishkek and LIDAR sites was equal to  $0.195 \pm 0.05$  and  $0.185 \pm 0.05$ , respectively. For PM<sub>2.5</sub>, the annual averaged surface concentrations were equal to  $11.65 \pm 3.7$  and  $9.95 \pm 3.4 \mu\text{g}/\text{m}^3$  at Bishkek and LIDAR, respectively. Photometric data varied from 0.02 to 1.6 throughout the study period. Hourly values of PM<sub>2.5</sub> at the surface ranged from  $1.5 \mu\text{g}/\text{m}^3$  to  $119.6 \mu\text{g}/\text{m}^3$ . Typical values of AOD<sub>500</sub> and PM<sub>2.5</sub> during the warm season varied from 0.1 to 0.2 and from 5 to  $25 \mu\text{g}/\text{m}^3$ , respectively. Seasonal changes of PM<sub>2.5</sub> were 20–40 % in cold months and 35–55 % during the warm period. Monthly averaged PM<sub>2.5</sub>, PMCoarse, and AOD<sub>500</sub> values measured from July 2008 to June 2009 at the two sites are shown in Figure 2.

In general the annual variability of PM and AOD were similar at both sites with maximum values of PM<sub>2.5</sub>, PMCoarse, and AOD occurring at the end of the summer - early autumn (August-September) and in the spring (March-April). These variations were mainly the result of seasonal factors and the impact of long-range transport of desert.

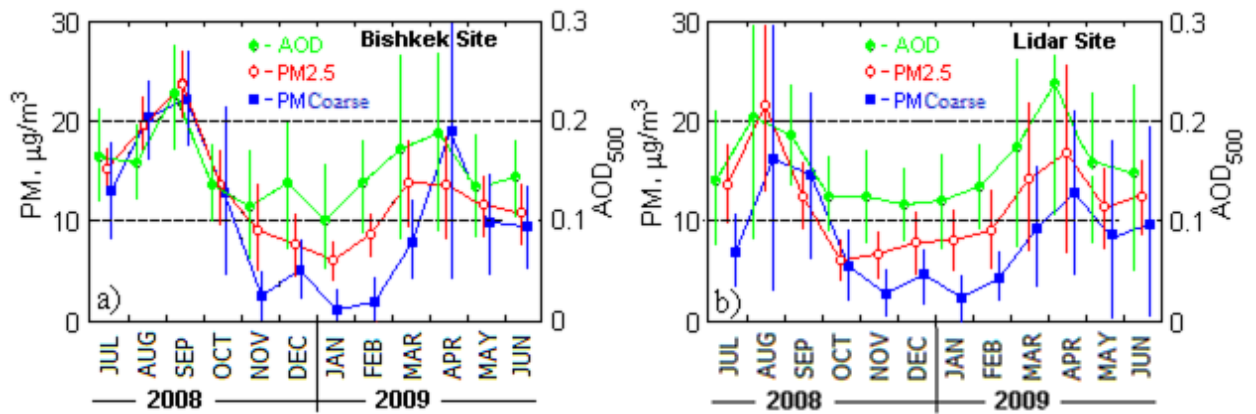


Figure 2. Monthly averaged values of PM<sub>2.5</sub>, PMCoarse, and AOD<sub>500</sub> at *Bishkek* (a) and *LIDAR* (b) sites.

Error bars correspond to  $\pm 1$  standard deviation.

Results for the year (177 sampling points) indicated a linear correlation between simultaneously measured concentration of PM<sub>2.5</sub> and PMCoarse (Figure 3A). At the LIDAR site the correlation was  $r^2 = 0.79$  (Figure 3A). Similar correlations were observed during dust episodes suggesting that dust transport is an important source of PM<sub>2.5</sub> and PMCoarse at these sites. The typical volumetric particle size distribution (Figure 3B) based on the photometric measurements (Cimel, AERONET, Issyk-Kul), shows that Asian dust contains a wide spectrum of particles with radii ranging from  $0.5 \mu\text{m}$  to  $10.0 \mu\text{m}$  significantly skewed towards coarse particle sizes. .

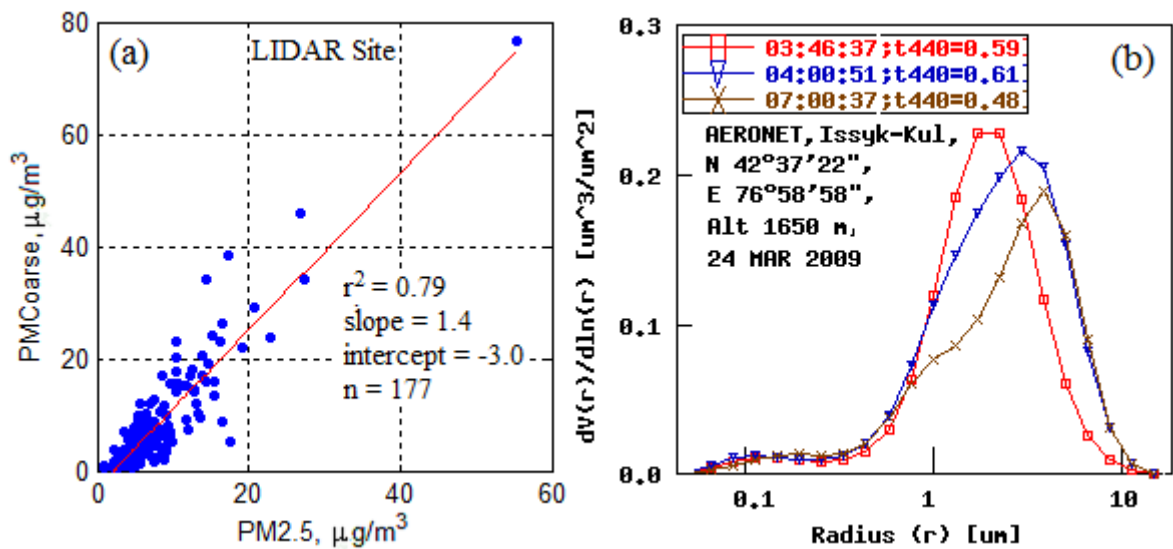


Figure 3. Relationship between PM<sub>2.5</sub> and PM<sub>Coarse</sub> at the *LIDAR* site (3A) and volumetric particles size distributions determined from the photometric data at Issyk-Kul station (AERONET) during a dust transport even on 24 March, 2009 (03:46 – 07:00 UTC) (3B).

Coarse particles not only dominate the size distribution during dust transport events but these events also influence PM<sub>2.5</sub> concentrations as observed in Figure 3a where PM<sub>c</sub> accounts for over 70% of the variation in PM<sub>f</sub>. The correlation between PM<sub>2.5</sub> and AOD<sub>500</sub> varied from season-to-season with the highest correlation coefficients corresponding to periods with the highest values of AOD<sub>500</sub> and PM<sub>2.5</sub> mass (see Figure 2). Regression coefficients for each season and the year are shown in Table 3.

Table 3. Linear regression statistics between daily averaged values of AOD<sub>500</sub> and PM<sub>2.5</sub> for each season and the whole year

Site	PM <sub>2.5</sub> vs. AOD <sub>500</sub>							
	Bishkek				LIDAR			
Parameter	n	a	b	r <sup>2</sup>	n	a	b	r <sup>2</sup>
Summer	59	63,9±9,7	5,7±2,0	0,39	56	43,7±6,7	5,3±1,3	0,44
Autumn	46	59,8±9,4	1,7±1,6	0,76	62	48,4±6,1	0,2±1,0	0,51
Winter	35	35,4±6,8	0,7±0,9	0,26	55	30,2±6,1	3,0±0,8	0,32
Spring	44	55,9±11,8	3,1±2,0	0,56	47	56,2±5,3	1,4±1,1	0,72
Annual	184	57,0±5,4	2,8±1,0	0,51	220	52,2±5,3	1,3±0,6	0,54

\* n = number of points, a = slope, b = intercept, r<sup>2</sup> = correlation coefficient

The lowest correlation at both sites, r<sup>2</sup>=0.26 (*Bishkek*) and r<sup>2</sup>=0.32 (*LIDAR*) occurred in the winter, when the contribution from local anthropogenic sources (e.g., coal combustion and biomass burning, diesel engines emissions) (Miller-Schulze et al., 2011) was the greatest and PM<sub>Coarse</sub> levels were the lowest. During this period monthly average PM<sub>Coarse</sub> values never exceeded 5 µg/m<sup>3</sup> whereas PM<sub>2.5</sub> values were greater than 5 µg/m<sup>3</sup> at both sites. Thus during the year different sources appear to impact the different size ranges with coarse particles having a larger influence on fine particle concentrations

during the dust transport seasons, while fine particles have little influence on coarse particles during the period when anthropogenic sources dominate. .

The highest correlations between AOD and PM<sub>2.5</sub> were observed in the spring, summer, and autumn and were mainly associated with dust transport events from the Taklimakan desert. During these seasons higher correlation coefficients were observed: 0.56, 0.39 and 0.76 (*Bishkek*) and 0.72, 0.44 and 0.51 (*LIDAR*). These results indicate that between 40 and 76% of the variability in AOD<sub>500</sub> during these seasons was due to variations in PM<sub>2.5</sub>. Strong correlations were observed between PM<sub>2.5</sub> and AOD<sub>500</sub> in autumn at the Bishkek site ( $r^2 = 0.76$ ) and in spring time at LIDAR site ( $r^2 = 0.72$ ) when aerosol particles were concentrated predominantly in the boundary layer as indicated based on LIDAR results. The majority of episodes were connected with transport of dust (desert crustal material) from the Taklimakan desert, located in NW China (Table 4). The latter was suggested based on comparisons with the NAAPS model (Christensen, 1997) and back-trajectory analysis (HYSPLIT-4) (Draxler and Hess, 1998).

Table 4. Number of measurement days (n) at Bishkek and LIDAR sites and number of registered episodes of dust transported from Taklimakan desert

Year	2008						2009					
	Month	Jul	Aug	Sep	Oct	Nov	Dec	Jan	Feb	Mar	Apr	May
n ( <i>Bishkek</i> )	22	18	21	15	10	8	12	15	14	13	17	19
n ( <i>LIDAR</i> )	24	9	23	21	18	13	26	16	18	13	16	23
<b>Dust events</b>	1	2	2	1	0	1	0	0	2	3	2	1

Comparison of all daily averaged data for the year (OBS) and corresponding predicted values (PRED) of PM<sub>2.5</sub> were calculated using the seasonal relationships between PM<sub>2.5</sub> and AOD<sub>500</sub> (Table 3) and are shown in Figure 4. These results can be used to estimate PM<sub>2.5</sub> concentrations from AOD values when PM<sub>2.5</sub> data are not available.

The data shown in Figure 4 were normalized relative to the regression line to express the distribution in terms of percent. The core of the distribution (95 % of total points) is located between the upper and bottom border of the sector. Outliers were examined and those that did not coincided in time with the sun photometer measurements were excluded. The transformed data set resulted in increased correlations coefficients at both Bishkek and LIDAR ( $r^2 = 0.67$  and  $r^2 = 0.71$ , respectively).

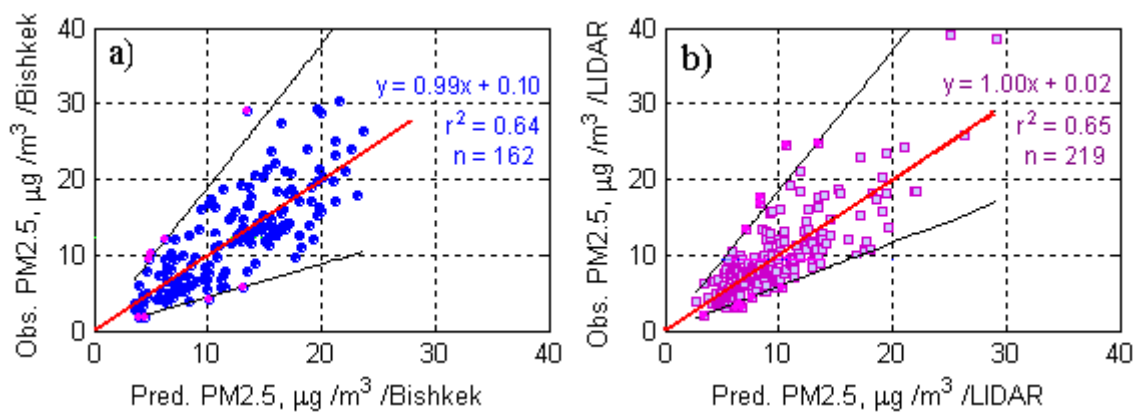


Figure 4. Dependence of measured (OBS) PM<sub>2.5</sub> and that estimated from optical measurements (PRED) at Bishkek (a) and LIDAR (b).

Table 5 displays the effect of time averaging on the correlation between AOD<sub>500</sub> and PM<sub>2.5</sub> and PMCoarse. More prolonged temporal averaging increases the correlation coefficients, with higher values for monthly averages of PM<sub>2.5</sub> and AOD<sub>500</sub>, than for daily and 1-hour averaged data. The results are similar to those reported in Natunen et al., (2010). Correlation coefficients between AOD<sub>500</sub> and PM<sub>2.5</sub> and PMCoarse were of the same order of magnitude (Table 5) since dust is not only a major component of PMCoarse, but also can cause a substantial increase in PM<sub>2.5</sub> mass due to the tail of the coarse particle size distribution extending into the fine fraction.

Table 5. Correlation coefficients ( $r^2$ ) for AOD<sub>500</sub> and PM<sub>2.5</sub> and PMCoarse at different averaging times

Site	Hourly average		Daily average		Monthly average	
	PM <sub>2.5</sub>	PMCoarse	PM <sub>2.5</sub>	PMCoarse	PM <sub>2.5</sub>	PMCoarse
<b>Bishkek</b>	0,41	–	0,51	0,50	0,67	0,60
<b>LIDAR</b>	0,47	–	0,54	0,59	0,73	0,78

Coarse particles have a slightly lower correlation with AOD than PM<sub>2.5</sub>, at the Bishkek site relative to the LIDAR site due to the impact of dust transported from the Taklimakan, since the LIDAR site is much closer to this desert than the Bishkek site. Using PMCoarse values instead of PM<sub>2.5</sub> in the comparison also leads to a decrease in the regression slope and negative intercept, indicating that coarse particles contribute less to AOD<sub>500</sub>, than to PM<sub>2.5</sub> (Koelemeijer et al., 2006).

### 3.2 Influence of boundary layer height and meteorology

Comparison of AOD and PM mass showed that the variability of AOD was not fully explained by the variability of PM possibly due to other factors, for example, variability in the vertical distribution of PM, meteorological parameters, and other properties of PM that might improve the correlation.

LIDAR data were used to estimate the influence of the atmospheric boundary layer height on the relationship between AOD and PM<sub>2.5</sub> at the LIDAR site. The PBL height, as measured by the LIDAR, has a seasonal variation from 1.0 to 4.0 km (Figure 5A). In general, AOD tends to track the height of the PBL

with lower values of both in the winter and higher values in the summer, consistent with trends in PM2.5 and PMCoarse.

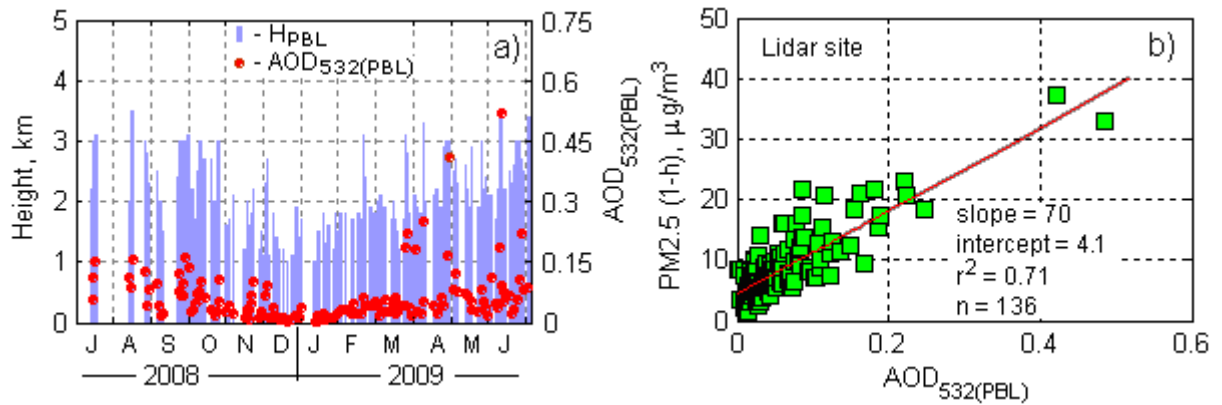


Figure 5. Annual variability of PBL height and LIDAR AOD (AOD<sub>532(PBL)</sub>) (5A) and comparison of hourly averages values of AOD<sub>532(PBL)</sub> and PM2.5 (5B).

For example, using the annual sun photometer dataset, taking into account the influence of the vertical distribution of the boundary layer by simple multiplication of PM2.5 by the PBL layer height (H<sub>PBL</sub>) gives a minor improvement in the correlation of PM2.5 with AOD from  $r^2 = 0.47$  to  $r^2 = 0.49$ .

The sun photometer only measures AOD during the day. However, the LIDAR can estimate AOD at night. To evaluate AOD during the nighttime, the correlation between AOD observed within the boundary layer (AOD<sub>532(PBL)</sub>) from the LIDAR and PM2.5 was calculated using a linear extrapolation of the lowest AOD value measured at 800 m to the ground. This extrapolation provided an integrated extinction over the entire PBL. This approach can lead to a small underestimation of AOD<sub>532(PBL)</sub> (Matthias and Bosenberg, 2002). Nevertheless, comparison of data averaged over 136 days resulted in a correlation coefficient ( $r^2$ ) of 0.58. A substantial improvement in the correlation ( $r^2 = 0.71$ ) was observed with the use of hourly averaged values of PM2.5 (Figure 5B) that coincided in time with the LIDAR measurements. Thus, estimating PM2.5 from AOD at night can be achieved from the LIDAR measurements.

Other factors, besides the vertical distribution of PM in the boundary layer can influence the relationship between AOD and PM. One factor is relative humidity (RH). Wang et al. (2010) described a method to account for the influence of both the height of the boundary layer and RH as indicated in equation 1.

$$PM_x = a_i \times AOD_\lambda / [H_{PBL} \times f(RH)] + b_i, \text{ where: } f(RH) = (1 - RH/100)^{-\xi}. \quad (\text{Eq. 1})$$

The correlation coefficient of PM and AOD only increased for the winter data ( $r^2 = 0.32$  to  $r^2 = 0.38$ ) at the LIDAR site. This can be explained by the dominance of anthropogenic PM2.5 observed during this period. Absence of an improvement in the correlation during the other seasons (especially in the spring)

likely reflects the low hygroscopic properties of dust found in PMCoarse (Van Donkelaar et al., 2009). Another source of uncertainty in the AOD-PM relationship is possibly due to the non-coincidence of MII and TEOM/FDMS measurements.

### 3.3 Correlation of AOD and PM<sub>2.5</sub> during dust intrusion

The measurement sites were located in a region that is typically impacted by dust transported from deserts several thousands of kilometers or more away from the sites (e.g., Aral Sea to the west, the Middle East to the far west, Gobi Desert to the NE, Taklimakan Desert to the SW). During the study, LIDAR measurements were able to identify several cases during the spring, summer, and autumn of mineral dust transport from deserts in the Middle East and the Taklimakan desert to the west. Identification of dust aerosol transport was verified based on ground-level AOD measurements (Bishkek and LIDAR sites), comparisons with the NAAPS model (Christensen, 1997), and based on back-trajectory analysis (HYSPLIT-4) (Draxler and Hess, 1998). Trajectories were assumed to contain dust if the bottom points of the trajectories were in the boundary layer over dust emission regions during these events. The identification of dust episodes also was verified based on an increase in PMCoarse ground-level concentrations, as a rule, PMCoarse exceeded PM<sub>2.5</sub> ( $PM_{2.5}/PM_{Coarse} < 1.0$ ) during these periods. The dominance of PMCoarse, reaching up to 70 % of the measured PM<sub>10</sub> mass, resulted in lower values of the Angstrom parameter ( $A_{380/870} < 0.7$ ) (Eck et al., 2005). Identified source regions included transport from the Tarim Basin in the Taklimakan desert in NW China, long-range transport of dust and anthropogenic aerosol from the direction of the Middle-East (Rodriguez et al., 2011), including the deserts of northeast Africa, Arabian Peninsula, and southwest Asia (Iraq, Iran, Afghanistan, Pakistan). Usually such events are characterized by high values of AOD and PM<sub>2.5</sub> and with durations from several hours to several days. One dust episode was observed during 07–11 August 2008 when 1-h average PM<sub>2.5</sub> concentrations reached  $120 \mu\text{g}/\text{m}^3$  and  $55 \mu\text{g}/\text{m}^3$  at the LIDAR and Bishkek sites, respectively. According to the NAAPS model there were dust storms during this period in northern (Gobi desert) and northwest China (Taklimakan desert), which impacted the LIDAR site (Figure 6).

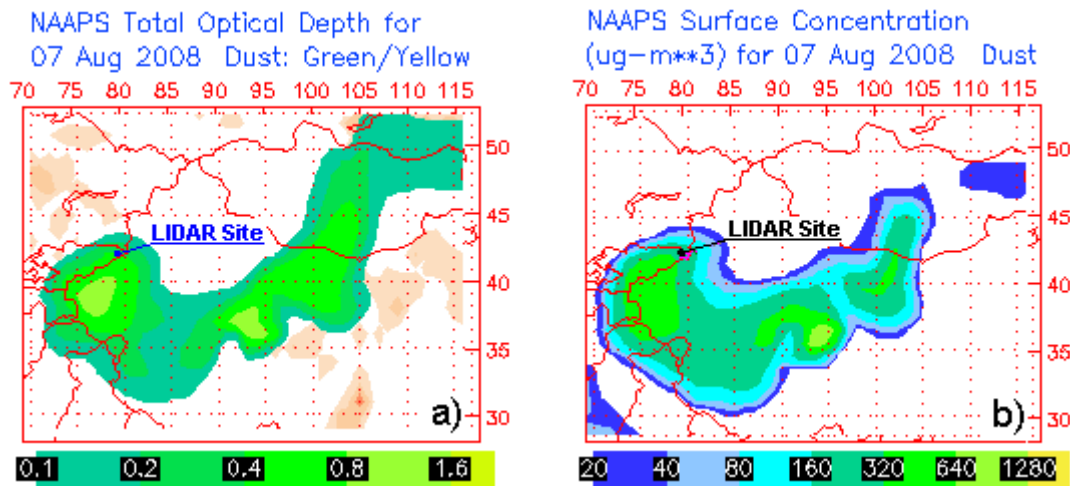


Figure 6. Distribution of total optical depth (6A) and surface dust concentration (6B), according to aerosol NAAPS model for 07 August 2008, 00:00UTC.

Based on LIDAR results the typical heights of the Asian dust layers were in the range of 1-4 km above ground level. Analysis of back trajectories to arrive at the LIDAR site at these altitudes indicated that dust particles were lifted into atmosphere in the Taklimakan desert and transported to the LIDAR site. As an example, Figure 7 shows results of back trajectories for 3.0 km above the LIDAR site. Dust transport time at this altitude did not exceed 48 hours as seen in Figure.

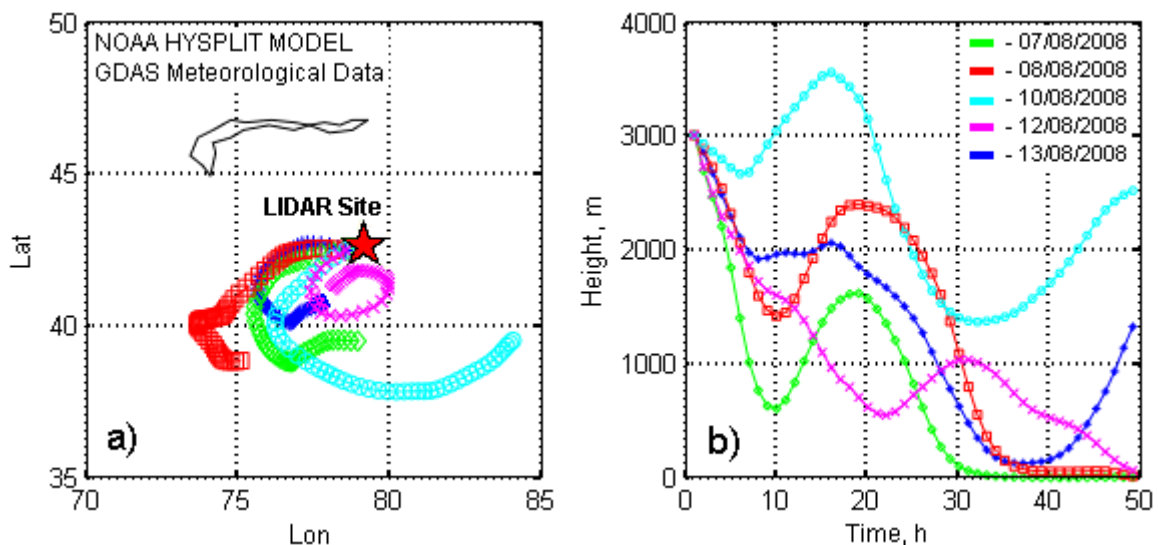


Figure 7. 48-h air-mass back-trajectories ending at LIDAR site at 14:00 UTC at level 3.0 km (a.g.l.) for the indicated dates.

The Angstrom parameter ( $A_{380/870}$ ), which characterizes the slope of the spectral dependence of AOD (Eck et al., 1999) and is related to the particle size distribution, was calculated using measured values of AOD at 380 and 870 nm wavelengths:  $A_{380/870} = -\ln(AOD_{380}/AOD_{870})/\ln(380/870)$ . Lower values of the Angstrom parameter suggest a greater influence from coarse particles (Soni et al. 2011). Observed  $AOD_{500}$ , Angstrom parameter, and  $PM_{2.5}$  mass concentrations observed at the LIDAR site during the

period of 05–15 August 2008 are shown in Figure 8A. Based on the  $A_{380/870}$  ( $A_{380/870} \leq 0.26$ ), it is clear that the lower end of the coarse particle size distribution impacts the PM<sub>2.5</sub> size range during this entire dust event.

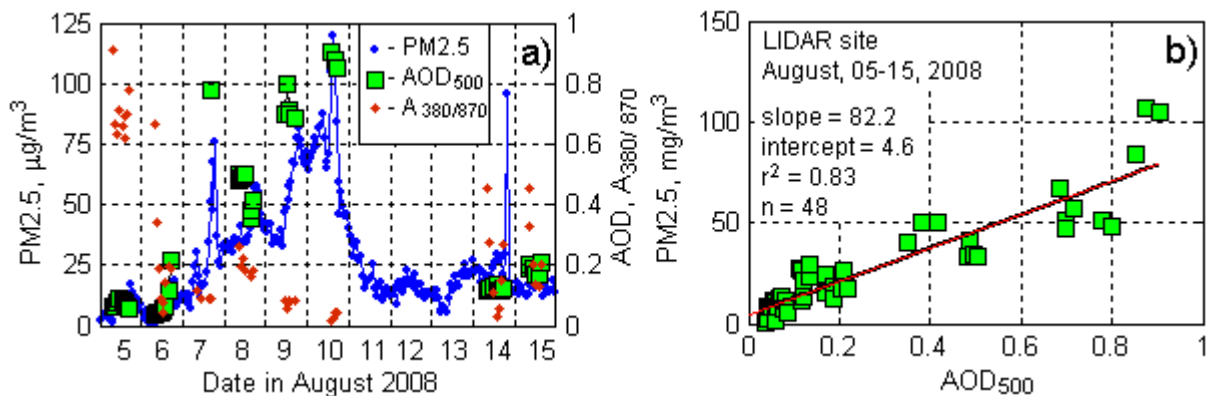


Figure 8. 1-hour average values of PM<sub>2.5</sub>, AOD<sub>500</sub> and A<sub>380/870</sub> (8A) and comparison of AOD<sub>500</sub> vs. PM<sub>2.5</sub> during August, 05–15, 2008 (8B).

Comparison of all 1-h averaged values of AOD<sub>500</sub> and PM<sub>2.5</sub> during the 05-15 August dust episode (Figure 8B) showed a high correlation ( $r^2 = 0.83$ ). In general, it should be noted that a good correlation between parameters was observed in the vast majority of Asian dust episodes and the correlation improved with increase in average values of AOD<sub>500</sub> and PM<sub>2.5</sub> mass concentrations. A similar behavior of optical thickness and mass concentration was observed by Gupta et al. (2006).

Based on these results, it appears possible to estimate the influence of Asian dust transported to the two sites based on the relationship observed between daily average AOD<sub>500</sub> and PM<sub>2.5</sub>. Data obtained during days when dust was transported from Taklimakan desert (Figure 9A) were selected for this comparison. Dark blue markers indicate daily average values at the LIDAR site, for which the correlation coefficient was  $r^2=0.80$ . The LIDAR site is located in relatively close proximity to the Taklimakan desert, and high values of average AOD<sub>500</sub> and PM<sub>2.5</sub> are observed, equal to  $0.40 \pm 0.21$  and  $30.3 \pm 16.2 \mu\text{g}/\text{m}^3$ , respectively. At the Bishkek site, a similar analysis (red markers) had a lower correlation ( $r^2=0.55$ ) with lower average values of AOD<sub>500</sub> and PM<sub>2.5</sub>, equal to  $0.26 \pm 0.08$  and  $23.5 \pm 6.1 \mu\text{g}/\text{m}^3$ , which indicates a smaller influence of Asian dust.

Therefore, examining the dependence of AOD<sub>500</sub> and A<sub>380/870</sub> (Figure 9B) provides insight into the optical properties and particle size distribution of Asian dust reaching the Bishkek and LIDAR sites. As can be seen in Figure 9, particle size distributions at the LIDAR site are likely characterized by the prevalence of coarse particles as seen by the average Angstrom parameter ( $A_{380/870} = 0.10 \pm 0.33$ ). A wider range of the A<sub>380/870</sub> (from 0.05 to 0.72) was observed at Bishkek and was in some cases indicative of a mixture of coarse dust particles with anthropogenic fine particles. This mixture also can be one of the reasons for a lower correlation between AOD<sub>500</sub> and PM<sub>2.5</sub> at the Bishkek site.

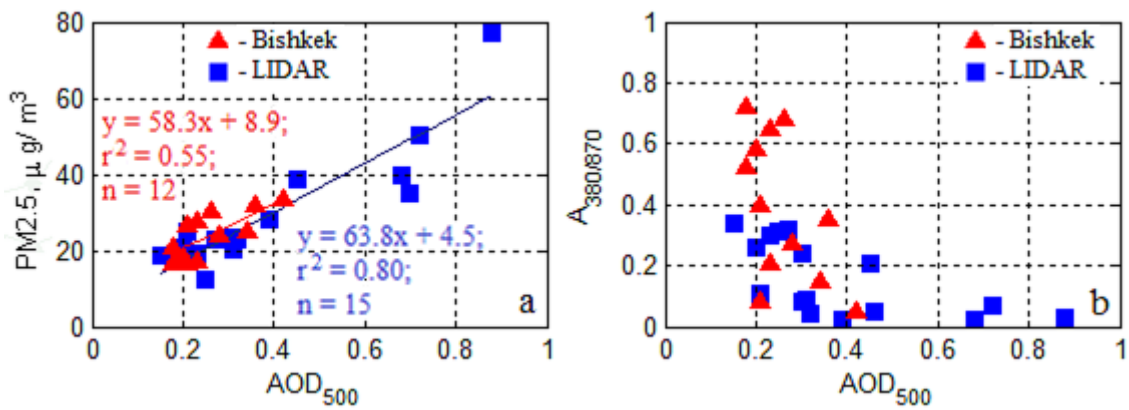


Figure 9. Comparison of results of AOD<sub>500</sub> and PM<sub>2.5</sub> measurements for all days identified as dust transported from Taklimakan desert (9A) and corresponding dependences of AOD<sub>500</sub> and A<sub>380/870</sub> (9B) at Bishkek and LIDAR sites.

The measured regression slopes (58.3 and 63.8  $\mu\text{g m}^{-3}/\text{unit AOD}$ ) are close to the values used for estimating PM<sub>2.5</sub> from AOD by the Moderate Resolution Imaging Spectroradiometer (MODIS) onboard of AQUA and TERRA satellites in the IDEA system (Infusing satellite Data into Environmental Applications). The MODIS value of 62  $\mu\text{g m}^{-3}/\text{unit AOD}$  is accepted as a constant for all regions and seasons (Zhang et al., 2009).

However, the relation between AOD and PM also is sensitive to aerosol types (Van Donkelaar et al., 2009). Therefore, in addition to days classified as dust events, other days without dust intrusion were examined and categorized. These periods primarily relate to pollution generated on a more local scale. Comparison of PM<sub>2.5</sub> and AOD for these periods is shown in Figure 10.

The factor of two difference in the slopes of  $\sim 32 \pm 2$  vs.  $\sim 61 \pm 3$   $\mu\text{g m}^{-3}/\text{unit AOD}$  on average of PM and AOD between the dust episodes and non-episode periods, respectively, can be explained by the larger contribution of fine particles to non-dust periods, which has a considerable impact on AOD, but only slightly impacts the PM<sub>2.5</sub> mass concentration (Qu et al., 2010).

Thus, it is necessary to consider the dominate type of aerosol (fine vs. coarse or dust vs. anthropogenic) when estimating PM concentrations based on MODIS AOD. Otherwise the estimate can lead to a considerable overestimation of PM values.

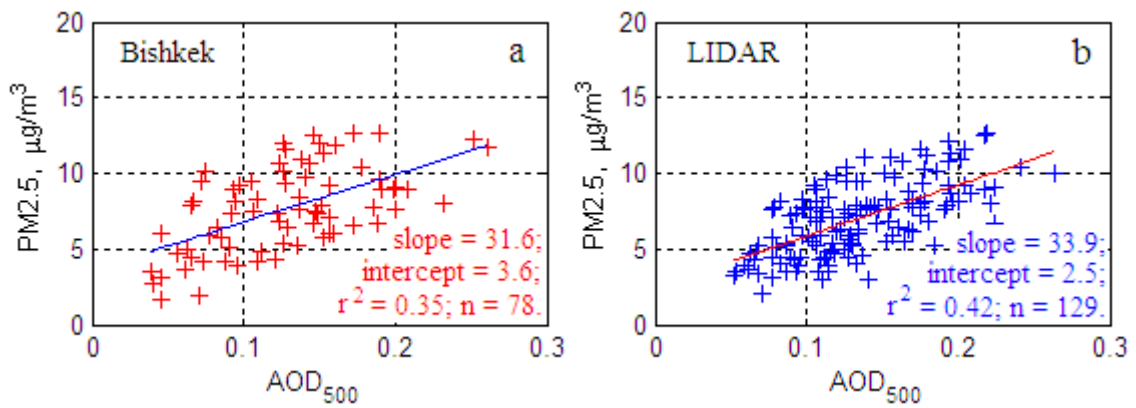


Figure 10. Comparison of AOD<sub>500</sub> and PM<sub>2.5</sub> measurement results, carried out in days without dust intrusion.

Results indicate that in the absence of dust (i.e., dust emitted from deserts) the air quality in the region is better than when impacted by dust transported from outside the region. For example, according to the US EPA, days can be categorized by good air quality when daily average PM<sub>2.5</sub> mass concentration is in the range from 0–15.4 µg/m<sup>3</sup> (Gupta et al., 2006). In this case, this occurs during days without dust intrusion. Days with dust intrusion, except for several cases, can be categorized as days with moderate air quality with PM concentrations ranging from 15.5 to 40.4 µg/m<sup>3</sup>.

When aerosol was transported from the Middle East, relatively high values of AOD<sub>500</sub> were usually accompanied by low concentrations of PM<sub>2.5</sub>. In these events, the dust layers were well above the PBL (from 4.0 to 8.0 km according to the LIDAR results) and did not heavily impact the ground layer (PM<sub>2.5</sub> = 8.5±4.6 µg/m<sup>3</sup>). This resulted in a weaker correlation between AOD<sub>500</sub> and PM<sub>2.5</sub> (r<sup>2</sup>=0.25÷0.35). Thus it is difficult to use the result of ground-based measurements to characterize dust transported from the Middle-East.

These results indicated that the relationship between PM<sub>2.5</sub> and AOD is variable during a yearly cycle and are strongly dependent on the source region of the aerosol; therefore, one regression equation cannot be used to predict PM<sub>2.5</sub> concentrations at the surface from AOD<sub>500</sub>. One approach is to account for these differences based on the magnitude of AOD<sub>500</sub> and A<sub>380/870</sub>. This resulted in two equations, one for background conditions (as a rule, during the winter period) when daily average values of AOD<sub>500</sub> were < 0.2 and A<sub>380/870</sub> > 0.7:

$$PM_{2.5(PRED)} = 32 \times AOD_{500} + 3.0 \text{ (}\mu\text{g/m}^3\text{)}$$

and during episodes, when dust within the boundary layer contributed to the aerosol loading (AOD<sub>500</sub> ≥ 0.2; A<sub>380/870</sub> < 0.7):

$$PM_{2.5(PRED)} = 60 \times AOD_{500} + 7.0 \text{ (}\mu\text{g/m}^3\text{)}.$$

These linear regression parameters correspond in general to values previously reported from ground-based (AERONET, <http://aeronet.gsfc.nasa.gov/>) and satellite (MODIS, <http://modis.gsfc.nasa.gov/>) AOD measurements and surfaced-based fine particle measurements (Wang and Christopher, 2003; Engel-Cox et al., 2004; Gupta et al., 2006), which were characterized by slopes and intercepts in the range from 22 to 77  $\mu\text{g}/\text{m}^3$  and from 5 to 12  $\mu\text{g}/\text{m}^3$ , respectively.

## Summary and Conclusions

Optical and physical characteristics of atmospheric particulate matter in the boundary layer were measured over a one-year period at two sites in Central Asia to evaluate the impact of local sources and long-range transport of dust into the region. The PM mass and composition measurements are unique to Central Asia. AOD, the optical metric was measured using a sun photometer. PM<sub>2.5</sub> mass concentrations were obtained using a semi-continuous sampler that provided hourly data throughout the study period. PM<sub>2.5</sub> and PM<sub>10</sub> mass and detailed chemical composition were measured on an every other day sampling schedule using a multi-filter sampler. Composition data are described elsewhere (e.g., Miller-Schulze et al., 2011).

AOD<sub>500</sub> and PM<sub>2.5</sub> day-time values ranged from 0.1 to 0.2 and from 5 to 25  $\mu\text{g}/\text{m}^3$ , respectively, during the warm season. Statistical analysis of all data showed a moderate relationship ( $r^2 = 0.41$  and  $r^2 = 0.47$ ) between AOD and hourly averaged values of PM<sub>2.5</sub>. Use of daily mean PM<sub>2.5</sub> data improved the correlation ( $r^2 = 0.54$  and  $r^2 = 0.61$ ) at the Bishkek and LIDAR sites, respectively. Results also indicated that transported dust from the surrounding deserts impacts the fine particle fraction influencing not only the seasonal dependence of the observed optical properties of the aerosol, but also leads to much higher correlation between PM<sub>2.5</sub> and AOD. Comparison of photometric measurements with coarse particle mass (PM<sub>10</sub>–PM<sub>2.5</sub>) showed lower correlation ( $r^2 = 0.50$ ) at Bishkek site, than at LIDAR site ( $r^2 = 0.59$ ), possibly, because of proximity of the latter to Taklimakan desert, which during our study period appeared to be one of the main sources affecting air quality at the sites, especially at the LIDAR site. In general, correlation coefficients and aerosol loading were higher at LIDAR site.

Estimates of PM<sub>2.5</sub> mass at the surface from sun photometer AOD measurements required the development of two regression equations accounting for the seasonal dependence and differences in atmospheric aerosol optical properties, which are influenced by differences in the sources of long-range transport of dust and anthropogenic pollutants. Simple linear dependences between daily average values of AOD<sub>500</sub> and PM<sub>2.5</sub> are presented during periods with dust transport and during days without dust intrusion using the criteria based on modeling, satellite, and experimental data. The following regression equations were obtained:  $\text{PM}_{2.5} = 32 \times \text{AOD}_{500} + 3.0$ , for daily average values of  $\text{AOD}_{500} < 0.2$ ;  $\text{A}_{380/870} > 0.7$ , typically during the winter when fine particles were dominant due to the impact of local

anthropogenic sources, and  $PM_{2.5} = 60 \times AOD_{500} + 7.0$ , for daily average values of  $AOD_{500} \geq 0.2$ ;  $A_{380/870} < 0.7$  when the sites were impacted by regional and long range dust transport. The factor of two difference in the slopes of regression lines between local pollution events vs. long range transport periods ( $\sim 32$  and  $\sim 62 \mu g m^{-3} / \text{unit AOD}$ ) should be taken into account when estimating the concentration of  $PM_{2.5}$  from satellite values of AOD.

Estimates of surface level  $PM_{2.5}$  mass also should be able to be obtained using LIDAR AOD obtained at night.

These results are in an agreement with previous of AOD and fine particle relationships observed in other parts of the world. The empirical relationships observed between AOD and  $PM_{2.5}$  can be used for estimating surface  $PM_{2.5}$  in previous years in Central Asia regions or in areas where no PM measurements have been made to establish subsequently the effects of air pollution influence on the environment and human health.

The results presented in the paper, are an initial stage of research examining the regional distribution of PM on the basis of satellite measurements (MODIS AOD), models, and surfaced based measurements of AOD and PM.

#### Acknowledgements

The U.S. Environmental Protection Agency through its Office of Research and Development funded this study and collaborated in the research described here under Contract EP-D-06-001 to the Pechan and Associates and as a component of the International Science & Technology Center (ISTC) project # 3715 (Transcontinental Transport of Air Pollution from Central Asia to the US), the latter funded by EPA's Office of International and Tribal Affairs and the Office of Science Policy. It has been subject to Agency review and approved for publication. Mention of trade names or commercial products does not constitute endorsement, certification, or recommendation for use.

#### REFERENCES

- Chen B.B., Sverdlik L.G., Kozlov P.V. (2004), Optics and microphysics of atmospheric aerosol, Bishkek, 222 P.
- Christensen, J. H. (1997), The Danish Eulerian hemispheric model – a three-dimensional air pollution model used for the arctic, Atmos. Environ., 31, 4169–4191.
- Dinoi A., Perrone M.R. and Burlizzi P. (2010), Application of MODIS Products for Air Quality Studies Over Southeastern Italy, Remote Sens., 2, 1767-1796; doi:10.3390/rs2071767.

Draxler R., Hess G. (1998), An overview of the HYSPLIT\_4 modeling system for trajectories, dispersion, and deposition, *Aust. Meteorol. Mag.*, 47, 295–308.

Eck, T. F., Holben, B. N., Reid, J. S., Dubovik, O., Smirnov, A., O'Neill, N. T., Slutsker, I., and Kinne, S. (1999), Wavelength dependence of the optical depth of biomass burning, urban, and desert dust aerosols, *J. Geophys. Res.*, 104, 31333–31349.

Engel-Cox J.A., Holloman C.H., Coutant B.W., and Hoff R.M. (2004), Qualitative and quantitative evaluation of MODIS satellite sensor data for regional and urban scale air quality, *Atmos. Environ*, 38, 2495–2509.

Federal Register. (2006). National Ambient Air Quality Standards for Particulate Matter: Final Rule. 40 CFR Parts 50, 53, and 58, Volume 62 (138). Part 50:

<http://www.epa.gov/ttn/amtic/files/ambient/pm25/pt5006.pdf>; Parts 53 and 58:

<http://www.epa.gov/ttn/amtic/files/ambient/pm25/092706sign.pdf>, last accessed October 2, 2012.

Fischer E.V., Hsu N.C., Jaffe D.A., Jeong M.J., and Gong S.L. (2009), A decade of dust: Asian dust and springtime aerosol load in the U.S. Pacific Northwest, *Geophysical Research Letters*, Vol. 36, L03821, 5 PP., doi:10.1029/2008GL036467.

Gupta P., Christopher S.A., Wang J., Gehrig R., Leed Y., Kumar N. (2006), Satellite remote sensing of particulate matter and air quality assessment over global cities, *Atmospheric Environment*, 40, P. 5880–5892.

Heo J.-B., Hopke P.K., and Yi S.-M. (2009), Source apportionment of PM<sub>2.5</sub> in Seoul, Korea, *Atmos. Chem. Phys.*, 9, 4957–4971.

Ho K.F., Lee S.C., Cao J.J., Li Y.S., Chow J.C., Watson J.G., and Fung K. (2006), Variability of organic and elemental carbon, water soluble organic carbon, and isotopes in Hong Kong, *Atmos. Chem. Phys.*, 6, 4569–4576.

Hoff R.M., Christopher S.A. (2009), Remote Sensing of Particulate Pollution from Space: Have We Reached the Promised Land, *J. Air & Waste Manage. Assoc.* 59:645–675.

Husar R.B., Tratt D.M., Schichtel B.A., Falke S.R., Li F., Jaffe D., Gassó S., Gill T., Laulainen N.S., Lu F., Reheis M.C., Chun Y., Westphal D., Holben B.N., Gueymard C., McKendry I., Kuring N., Feldman G.C., McClain C., Frouin R.J., Merrill J., DuBois D., Vignola F., Murayama T., Nickovic S., Wilson W.E., Sassen K., Sugimoto N., Malm W.C. (2001), The Asian dust events of April 1998. *J. Geophys. Res. – ATM* 106 (D16), 18317-18330.

Ichoku, C., R. Levy, Y.J. Kaufman, L.A. Remer, R.-R. Li, V.J. Martins, B.N. Holben, N. Abuhassan, I. Slutsker, T.F. Eck, and C. Pietras. (2002), Analysis of the performance characteristics of the five-channel Microtops II Sun photometer for measuring aerosol optical thickness and precipitable water vapor, *J. Geophys. Res.*, Vol.107, No D13, 4179.

Kacenenbogen M., L'eon J.-F., Chiapello I., and Tanre D. (2009), Characterization of aerosol pollution events in France using ground-based and POLDER-2 satellite data, *Atmos. Chem. Phys.*, 6, 4843–4849.

Koелеmeijer R.B.A., Schaap M., Timmermans R.M.A., Homan C.D., Matthijsen J., Van de Kassteele J., and Builtjes P.G.H. (2006), Mapping aerosol concentrations and optical thickness over Europe – PARMA final report", MNP report 555034001, Bilthoven, the Netherlands.

Kokhanovsky A.A., Glantz P., von Hoyningen-Huene W., Burrows J.P. (2008), The Determination of Aerosol Optical Thickness and Particulate Matter Concentration Using Satellite Observations, *Geophysical Research Abstracts*, Vol. 10, EGU2008-A-03005.

Kumar N., Chu A., and Foster A. (2007), An empirical relationship between PM<sub>2.5</sub> and aerosol optical depth in Delhi Metropolitan, *Atmos. Environ.*, 41, 4492–4503.

Kuśmierczyk-Michulec J. (2010), Optical Measurements of Atmospheric Aerosols in Air Quality Monitoring, *Optical Measurements of Atmospheric Aerosols in Air Quality Monitoring, Air Quality - Models and Applications*, Ch.9, 153-172.

Lee H.N., Igarashi Y., Chiba M., Aoyama M., Hirose K., Tanaka T. (2006), Global model simulations of the transport of Asian and Sahara Dust: total deposition of dust mass in Japan. *Water, Air, and Soil Pollution*, 169, 137-166.

Lee Y.C., Yang X., Wenig M. (2010), Transport of dusts from East Asian and non-East Asian sources to Hong Kong during dust storm related events 1996-2007. *Atmospheric Environment*, 44, 3728-3738.

Liu D., Wang Z., Liu Z., Winker D., Trepte C. (2008), A height resolved global view of dust aerosols from the first year CALIPSO lidar measurements. *J. Geophys. Res.*, 113, D16214.

Matthias V., Bosenberg J. (2002), Aerosol climatology for the planetary boundary layer derived from regular lidar measurements, *Atmos. Research*, 63, 221–245.

McKendry I.G., Strawbridge K.B., O'Neill N.T., Macdonald A.M., Liu P.S.K., Leaitch W.R., Anlauf K.G., Jaegle L., Fairlie T.D., and Westphal D.L. (2007), Trans-Pacific transport of Saharan dust to western North America: A case study. *J. Geophys. Res.*, Vol. 112, D01103, doi:10.1029/2006JD007129.

- Miller-Schulze, J.P., Shafer, M. Schauer, J.J., Solomon, P.A., Lantz J.J., Artamonova M., Chen B., Imashev S., Sverdlik L., Carmichael G., and Deminter J. (2011), Characteristics of Fine Particle Carbonaceous Aerosol at Two Remote Sites in Central Asia. *Atmos. Environ.* 45(38), 6955-6964.
- Mukai S., Sano I., Mukai M., and Yasumoto M. (2008), Evaluation of air quality from space, *Proceedings of SPIE – The International Society for Optical Engineering*, 6745, 67451X.1–67451X.8.
- Natunen A., Arola A., Mielonen T., Huttunen J., Komppula M. and Lehtinen K.E.J. (2010), A multi-year comparison of PM<sub>2.5</sub> and AOD for the Helsinki region. *Boreal Env. Res.* 15: 544–552.
- Park C.B., Sugimoto N., Matsui I., Shimizu A., Tatarov B., Kamei A., Lee C.H., Uno I., Takemura T., Westphal D.L. (2005), Long-range Transport of Saharan Dust to East Asia Observed with Lidars. *SOLA*, Vol. 1, pp. 121-124.
- Pelletier B., Santer R., and Vidot J. (2007), Retrieving of particulate matter from optical measurements: A semiparametric approach, *J. Geophys. Res.*, Vol. 112, D06208, doi:10.1029/2005JD006737.
- Pope III C.A. and Dockery D.W. (2006), Health Effects of Fine Particulate Air Pollution: Lines that Connect, *J. Air Waste Manage. Assoc.*, 56, 709–742.
- Qu W.J., Arimoto R., Zhang X.Y., Zhao C.H., Wang Y.Q., Sheng L.F., and Fu G. (2010), Spatial distribution and interannual variation of surface PM<sub>10</sub> concentrations over eighty-six Chinese cities *Atmos. Chem. Phys.*, 10, 5641–5662.
- Rodriguez S., A. Alastuey, S. Alonso-Perez, X. Querol, E. Cuevas, J. Abreu-Afonso, M. Viana, N. Perez, M. Pandolfi, and J. de la Rosa. (2011), Transport of desert dust mixed with North African industrial pollutants in the subtropical Saharan Air Layer, *Atmos. Chem. Phys.*, 11, 6663–6685.
- Schaap M., Apituley A., Timmermans R.M.A., Koelemeijer R.B.A., and De Leeuw G. (2009), Exploring the relation between aerosol optical depth and PM<sub>2.5</sub> at Cabauw, the Netherlands, *Atmos. Chem. Phys.*, 9, 909–925.
- Smirnov A., Holben B.N., Slutsker I., Giles D.M., McClain C.R., Eck T.F., Sakerin S.M., Macke A., Croot P., Zibordi G., Quinn P.K., Sciare J., Kinne S., Harvey M., Smyth T.J., Piketh S., Zielinski T., Proshutinsky A., Goes J.I., Nelson N.B., Larouche P., Radionov V.F., Goloub P., Krishna Moorthy K., Matarrese R., Robertson E.J., and Jourdin F. (2009), Maritime Aerosol Network as a component of Aerosol Robotic Network, *J. Geophys. Res.*, 114, D06204.

Solomon, P.A.; Sioutas, C. (2008) Continuous and Semicontinuous Monitoring Techniques for Particulate Matter Mass and Chemical Components: A Synthesis of Findings from EPA's Particulate Matter Supersites Program and Related Studies; J. Air & Waste Manage. Assoc., 58(2), 164–195.

Solomon P.A. (2011), Air Pollution and Health: Bridging the Gap from Sources to Health Outcomes. Environ Health Perspect. 119(4): 156–157.

Soni K., Singh S., Bano T., Tanwar R.S., and Nath S. (2011), Wavelength dependence of the aerosol angstrom exponent and its implications over Delhi, India, Aerosol Sci. Technol., 45, 12, 1488-1498.

United Nations Environment Programme: Global Deserts Outlook (2006), UNEP Job No. DEW/0839/NA.

Van Donkelaar A.; Martin R.V.; Brauer M., Kahn R., Levy R., Verduzco C. and Villeneuve P.J. (2009), Global Estimates of Ambient Fine Particulate Matter Concentrations from Satellite-Based Aerosol Optical Depth: Development and Application, Environmental Health Perspectives, Volume: 118, Issue: 6, Pages: 847–855.

Wang J. and Christopher S.A. (2003), Intercomparison between satellite derived aerosol optical thickness and PM<sub>2.5</sub> mass: implications for air quality studies, Geophys. Res. Lett., 30 (21), 2095.

Zhang H., Hoff R.M., Engel-Cox J.A. (2009), The Relation between Moderate Resolution Imaging Spectroradiometer (MODIS) Aerosol Optical Depth and PM<sub>2.5</sub> over the United States: A Geographical Comparison by U.S. Environmental Protection Agency Regions, J. Air & Waste Management Association Volume 59:1358–1369 DOI:10.3155/1047-3289.59.11.1358.

#### Figure Captions

Figure 1. Location of the LIDAR and Bishkek monitoring sites.

Figure 2A and 2B. Monthly averaged values of PM<sub>2.5</sub>, PM<sub>Coarse</sub> and AOD<sub>500</sub> at Bishkek (2A) and LIDAR (2B) sites. Error bars correspond to ±1 standard deviation.

Figure 3. Relationship between PM<sub>2.5</sub> and PM<sub>Coarse</sub> at the LIDAR site (3A) and volumetric particles size distributions determined from the photometric data at Issyk-Kul station (AERONET) during a dust transport even on 24 March, 2009 (03:46 – 07:00 UTC) (3B).

Figure 4A and 4B. Dependence of observed PM<sub>2.5</sub>(OBS) and PM<sub>2.5</sub>(PRED) predicted from AOD measurements at : Bishkek (4A) and LIDAR (4B).

Figure 5A and 5B. Annual variability of height (H<sub>PBL</sub>) and lidar optical depth of atmospheric boundary layer AOD<sub>532(PBL)</sub> (5A) and comparison of hourly averages values of AOD<sub>532(PBL)</sub> and PM<sub>2.5</sub> (5B).

Figure 6A and 6B. Distribution of total optical depth (6A) and surface dust concentration (6B), according to aerosol NAAPS model for 07 August 2008, 00:00UTC.

Figure 7. 48-h air-mass back-trajectories ending at LIDAR site at 14:00 UTC at level 3.0 km (a.g.l.) for the indicated dates.

Figure 8A and 8B. 1-hour average values of PM<sub>2.5</sub>, AOD<sub>500</sub> and A<sub>380/870</sub> (8A) and comparison of AOD<sub>500</sub> vs. PM<sub>2.5</sub> during period of August, 05–15, 2008 (8B).

Figure 9A and 9B. Comparison of results of AOD<sub>500</sub> and PM<sub>2.5</sub> measurements for all days identified as dust transported from Taklimakan desert (9A) and corresponding dependences of AOD<sub>500</sub> and A<sub>380/870</sub> (9B) at *Bishkek* and *LIDAR* sites.

Figure 10. Comparison of AOD<sub>500</sub> and PM<sub>2.5</sub> measurement results, carried out in days without dust intrusion.

Supporting Information for:

Empirical Relationship between PM<sub>2.5</sub> and Aerosol Optical Depth over Northern Tien-Shan

Boris B. Chen <sup>(a)\*</sup>

Leonid G. Sverdlik <sup>(a)</sup>

Sanjar A. Imashev <sup>(a)</sup>

Paul A. Solomon <sup>(b)</sup>

Jeffrey Lantz <sup>(c)</sup>

James J. Schauer <sup>(d)</sup>

Martin M. Shafer <sup>(d)</sup>

Maria S. Artamonova <sup>(e)</sup>

Greg Carmichael <sup>(f)</sup>.

(a) Kyrgyz-Russian Slavic University, 44 Kievskaya Str., Bishkek 720000, Kyrgyz Republic,

(b) U.S. EPA, Office of Research & Development, Las Vegas, NV 89119 USA,

(c) U.S. EPA, Office of Radiation and Indoor Air, Las Vegas, NV 89119 USA,

(d) Wisconsin State Laboratory of Hygiene, University of Wisconsin, 660 North Park St, Madison, WI 53706, USA, Environmental Chemistry and Technology Program, 660 North Park St, University of Wisconsin, Madison 53706, USA,

(e) Institute of Atmospheric Physics, 109017 Moscow, Russia,

(f) Department of Chemical & Biochemical Engineering, the University of Iowa, Iowa City, IA 52242.

\*: Corresponding Author:

Email: [lidar@istc.kg](mailto:lidar@istc.kg)

Address: Kyrgyz-Russian Slavic University, 44 Kievskaya Str., Bishkek 720000, Kyrgyz Republic

Telephone: 996-312-431-197

Fax: 996-312-431-171